

Aberrant activity of the DNA repair enzyme AlkB

Timothy F. Henshaw^a, Michael Feig^{a,b}, Robert P. Hausinger^{b,c,*}

^a Department of Chemistry, Michigan State University, East Lansing, MI 48824-4320, USA

^b Department of Biochemistry and Molecular Biology, 4223 Biomedical Physical Sciences Building, Michigan State University, East Lansing, MI 48824-4320, USA

^c Department of Microbiology and Molecular Genetics, 6193 Biomedical Physical Sciences Building, Michigan State University, East Lansing, MI 48824-4320, USA

Received 18 September 2003; received in revised form 27 October 2003; accepted 31 October 2003

Abstract

Escherichia coli AlkB is a DNA/RNA repair enzyme containing a mononuclear Fe(II) site that couples the oxidative decomposition of α -ketoglutarate (α KG) to the hydroxylation of 1-methyladenine or 3-methylcytosine lesions in DNA or RNA, resulting in release of formaldehyde and restoration of the normal bases. In the presence of Fe(II), α KG, and oxygen, but the absence of methylated DNA, AlkB was found to catalyze an aberrant reaction that generates a blue chromophore. The color is proposed to derive from Fe(III) coordinated by a hydroxytryptophan at position 178 as revealed by mass spectrometric analysis. Protein structural modeling confirms that Trp 178 is reasonably positioned to react with the Fe(IV)-oxo intermediate proposed to form at the active site.

© 2003 Elsevier Inc. All rights reserved.

Keywords: DNA repair; AlkB; α -Ketoglutarate; Non-heme iron; Dioxygenase; Mass spectrometry; Protein modeling

1. Introduction

AlkB is an *Escherichia coli* DNA (and RNA) repair enzyme that protects the cell from the toxic effects of several methylating agents [1]. The enzyme catalyzes oxidative *N*-demethylation at 1-methyladenosine and 3-methylcytosine to remove the aberrant methyl groups as formaldehyde (Fig. 1) and restore the undamaged bases in DNA [2,3] and RNA [4]. Humans possess three homologues of AlkB, two that catalyze DNA repair activity [5] (including one that repairs methylation damage to RNA [4]) and a third of unknown function.

AlkB and its human homologues belong to a family of enzymes known as the iron(II)- and alpha-ketoglutarate (α KG)-dependent dioxygenases [6]. Like other family members, they activate dioxygen at a redox-active mononuclear center and abstract a hydrogen atom from a chemically non-reactive C–H bond to initiate

transformations that can include hydroxylations, ring closures, desaturations, and other reactions. An additional key feature of most of these enzymes is their ability to couple the oxidative decarboxylation of α KG to oxygen reduction; thus generating a putative Fe(IV)-oxo intermediate. Evidence for the production of an Fe(IV) intermediate was obtained in another family member, taurine/ α KG dioxygenase (TauD) [7], and model studies have demonstrated that Fe(IV)-oxo species can be generated at a mononuclear site [8,9]. Also consistent with the intermediacy of an Fe(IV)-oxo species is the finding of enzyme self-hydroxylation reactions in other family members [10–12]. For example, in the presence of α KG, but absence of taurine, TauD oxidizes Tyr 73 located near the active site to form a tyrosyl radical that converts to a catechol [11]. Coordination of the catechol side chain to the oxidized metal site creates greenish-brown (λ_{\max} 550 nm; $\epsilon_{550} \sim 700 \text{ M}^{-1} \text{ cm}^{-1}$) or green (λ_{\max} 700 nm; $\epsilon_{700} \sim 380 \text{ M}^{-1} \text{ cm}^{-1}$) ligand-to-metal charge-transfer (LMCT) chromophores, depending on whether bicarbonate is present [11,12]. Similarly, in the absence of its primary substrate

* Corresponding author. Tel.: +1-517-355-6463x1610; fax: +1-517-353-8957.

E-mail address: hausinge@msu.edu (R.P. Hausinger).

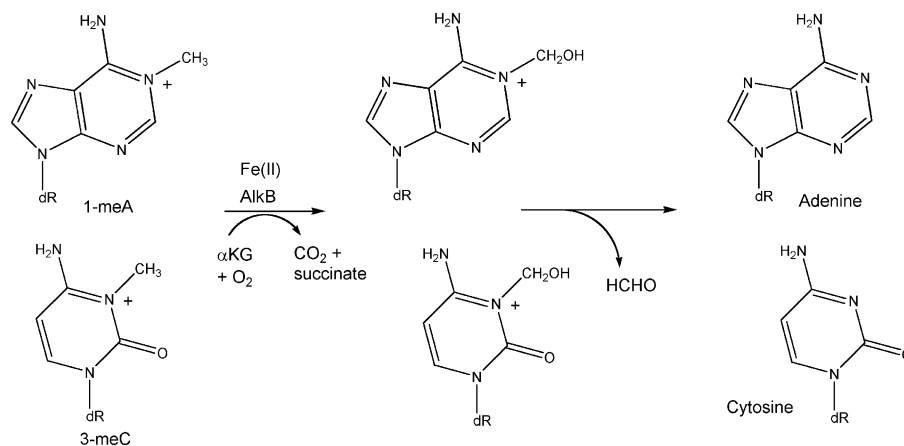


Fig. 1. DNA/RNA repair reaction catalyzed by AlkB.

2,4-dichlorophenoxyacetic acid (2,4-D), but presence of α KG, the 2,4-D/ α KG dioxygenase TfdA hydroxylates Trp 113, a residue located adjacent to a metal ligand of this protein [10]. Coordination of the hydroxytryptophan (OH-Trp) to the oxidized metalcenter yields a blue chromophore (λ_{max} 580 nm; $\epsilon_{580} \sim 1000 \text{ M}^{-1} \text{ cm}^{-1}$). These self-hydroxylation reactions are likely to arise from side reactions of the highly activated Fe(IV)-oxo species.

In this study, we provide evidence that AlkB also catalyzes self-oxidation of an amino acid side chain when incubated with Fe(II), α KG, and oxygen in the absence of its primary substrate, methylated DNA/RNA. This hydroxylated residue coordinates the oxidized metal site to produce a blue chromophore, analogous to that observed in TfdA. On the basis of mass spectrometric evidence, we identify the modification as hydroxylated Trp 178. Modeling of the AlkB structure provided evidence that Trp 178 is appropriately positioned near the metalcenter to undergo the observed oxidation chemistry.

2. Experimental

2.1. Sample preparation

His-tagged AlkB was overproduced in *E. coli* BL21(DE3) [pBAR54] and purified as previously described [2,13]. Significantly, cell disruption was carried out in buffers containing ethylenediaminetetraacetic acid (EDTA) to chelate the Fe(II) that is weakly bound to the enzyme and minimize any oxidative damage to the protein sample during purification.

2.2. UV-Visible (UV-Vis) spectroscopy

A cuvette containing 500 μ l of AlkB (240 μ M protein in 50 mM Hepes buffer, pH 8.0, with 300 mM NaCl) was made anaerobic by several rounds of vacuum and argon

on an anaerobic Schlenk line. Ferrous ammonium sulfate was added from an anaerobic stock (10 mM) to a final concentration of 200 μ M. α KG was added to a concentration of 1 mM. The enzyme was oxidized at room temperature ($\sim 23 \text{ }^\circ\text{C}$) by the addition of 300 μ l of water that had been saturated with O₂ at atmospheric pressure. The headspace of the cuvette was replaced with pure O₂. UV-Vis spectra were recorded at times indicated in the figure using a Beckman DU 7500 diode array spectrophotometer.

2.3. Mass spectrometry (MS)

AlkB samples were extensively dialyzed, diluted to a concentration of 1 nmol in 50 μ l of 100 mM ammonium bicarbonate buffer (pH 8.0), digested overnight with sequencing-grade modified trypsin (Promega) (1:40 molar ratio) at 37 $^\circ\text{C}$, and analyzed by nanoscale liquid chromatography mass spectrometry/mass spectrometry (LC/MS/MS). Five hundred fmol aliquots were applied to a picofrit column (75 μ m i.d. \times 5 cm) packed with 3 μ m Magic C-18 material (Micron Bioresources). Mobile phase A consisted of 0.1% formic acid while mobile phase B consisted of 0.1% formic acid in 90/10 acetonitrile/water. Peptides were eluted during a 25 min gradient extending from 2% to 60% B. The picofrit column made electrical contact through a pre-column ZDV titanium union, terminating in a 8 μ m tip i.d. outlet spray needle. Mass spectra were acquired by data dependent analysis in a Micromass Q-TOF Ultima mass spectrometer, where peptide ions detected in the MS survey scans triggered MS/MS fragmentation for obtaining product ion spectra. In order to identify peptides in the digest, the Mascot search engine was used to search the AlkB sequence.

2.4. Structural modeling

The structure for *E. coli* AlkB was predicted based on fold recognition in a functionally related oxidoreductase

(deacetoxycephalosporin C synthase from *Streptomyces clavuligerus*) where the structure is available from crystallography (PDB codes: 1DCS and 1RXG). This structure was identified as the best template with the Bioinfo Meta Server (<http://bioinfo.pl/Meta>) [14]. The alignment of secondary structure elements, as generated with the ORFeus method [15], was used to generate a structure scaffold by comparative modeling, where side chains in the template structure are replaced with the corresponding amino acids in *E. coli* AlkB. Connecting loops and other missing fragments were then added with the MMTSB Tool Set [16] by sampling conformational space with a low-resolution lattice model [17] and selecting the most favorable conformation based on clustering and an all-atom energy scoring function [18]. The position of the α KG ligand and Fe(II) were copied from the 1RXG crystal structure where the ligands were present. The complete structure including the ligand and iron was then minimized for 1000 steps with the molecular mechanics program CHARMM [19] under harmonic restraints to keep backbone and C β atoms near their initial positions. The ligand and iron were fixed during the minimization.

3. Results and discussion

3.1. Chromophore formation

The addition of α KG and Fe(II) to AlkB under anaerobic conditions generates a weak metal-to-ligand charge-transfer (MLCT) absorption at 450–500 nm [2]. When mixed with oxygen-saturated water, the pink color associated with this species disappeared and was replaced by a more intense blue chromophore (ϵ_{590} 960 M⁻¹ cm⁻¹ on the basis of iron concentration) with an absorption centered at 595 nm (Fig. 2). The slow color transformation occurred in two phases, with the relatively rapid disappearance of the α KG/Fe(II) chromophore (note the decrease in absorption at \sim 500 nm) preceding the increase of the 595 nm absorption. Full development of the blue chromophore required more than 10 min and followed an approximate first-order process (0.36 ± 0.05 min⁻¹ when measured starting at 2 min). Incubation of the sample under vacuum and exchange with an anaerobic atmosphere did not affect the blue color. Addition of dithionite to reduce the sample led to protein precipitation. In contrast to the situation for α KG/Fe(II)AlkB, no color was generated when Fe(II)AlkB lacking α -keto acid was mixed with oxygen-saturated water. The behavior observed here for AlkB and the resulting 595 nm spectrum are very similar to what was previously reported for TfdA, where the chromophore was attributed to the development of a LMCT transition involving OH-Trp coordinated to Fe(III) [10].

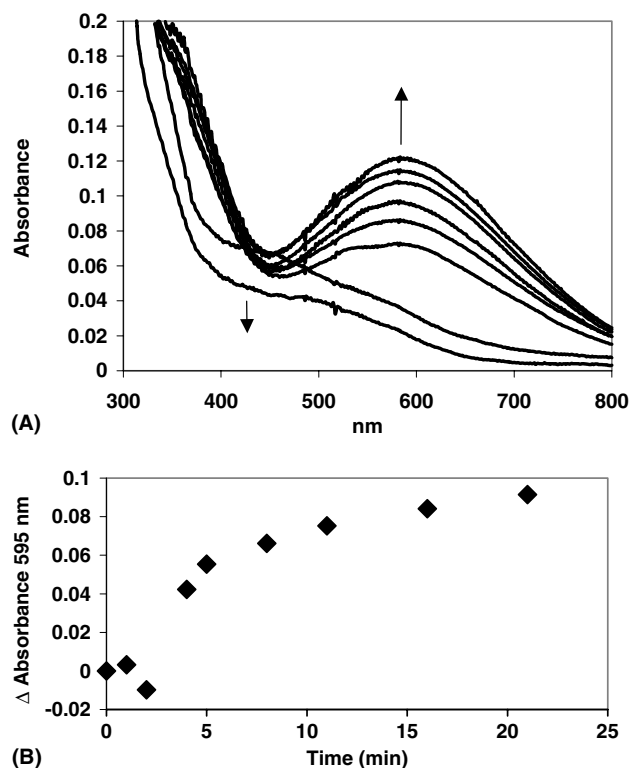


Fig. 2. UV-Visible spectroscopic analysis of the reaction of α KG-Fe(II)AlkB with oxygen. The Fe(II)- and α KG-bound form of AlkB was mixed with O₂-saturated water and spectra were recorded as a function of time. Panel A shows the loss of the MLCT absorption near 500 nm associated with the Fe(II)/ α KG center and the development of an intense visible chromophore centered at 595 nm. The kinetics of the spectral changes at 590 nm are illustrated in Panel B.

3.2. Mass spectrometric analysis

A hydroxylated Trp side chain of AlkB was identified by nanoscale capillary LC/MS/MS analysis. In this analysis, AlkB samples were first extensively dialyzed, diluted into ammonium bicarbonate (a volatile buffer), and digested with trypsin before injection. This method allows for very accurate and sensitive determinations of post-translationally modified amino acids within a protein. Using this approach, clear evidence was obtained for hydroxylation of a Trp side chain at position 178 (with numbering on the basis of the translated gene sequence). Product ion spectra revealed that all fragments containing Trp 178 were shifted by 16 Da and fragments not containing Trp 178 were unshifted (Fig. 3). Surprisingly, similar analyses revealed the presence of the same modification in a tryptic peptide of the control sample. This result is consistent with at least a portion of the overproduced AlkB undergoing modification during cell growth. We interpret the finding of Trp 178 hydroxylation as evidence that an Fe(IV)-oxo, or similarly reactive species, is generated in the reaction of α KG-Fe(II)AlkB with O₂ in the absence of methylated DNA

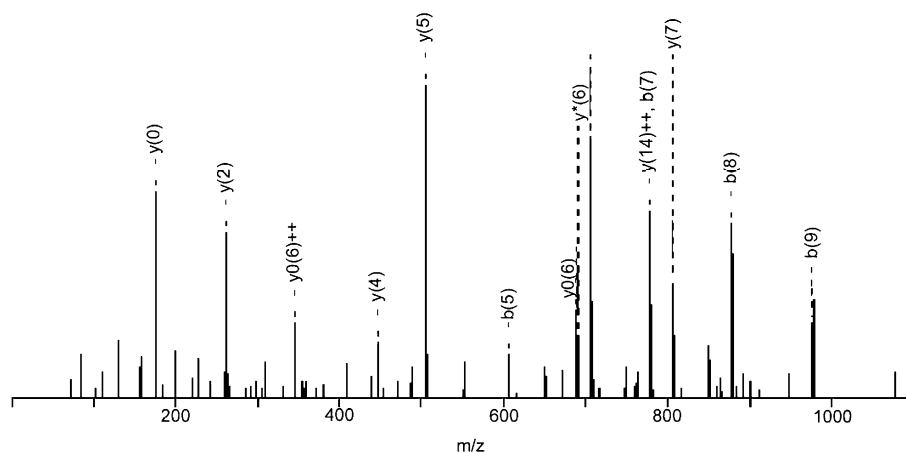


Fig. 3. LC/MS/MS identification of hydroxy-Trp 178 in AlkB. Tryptic peptides derived from oxygen-exposed α KG-Fe(II)AlkB were resolved by HPLC and analyzed by tandem MS/MS. The figure depicts the observed secondary MS product ions (mono- and di-protonated) derived from fragmentation of a parent ion (mass of 1780.91) associated with a single tryptic peptide. B ions are amino-terminal fragments and Y ions include the carboxyl terminal fragments. The parent ion and product ion masses match the sequence LLEHGDVVVWGGESR (residues 168–183 of AlkB) with a mass addition of 16 Da starting on the B11 and Y6 product ions. This 16 Da mass addition was consistent with the presence of hydroxy-Trp at residue 178.

substrate. Oxidation of the nearby Trp initiates the eventual formation of the hydroxy-Trp feature observed in the mass spectral analysis.

3.3. Protein modeling

An overview of the predicted structure for *E. coli* AlkB is shown in Fig. 4(A). It features the same double-stranded beta-helix and jelly-roll topology as the deacetoxycephalosporin C synthase templates used to build the model. Residues 1–15 are not shown since the prediction of the amino terminus is considered less reliable for the lack of a suitable template. The closeup view shown in Fig. 4(B) focuses on the immediate environment of the Fe(II) binding site. As expected, His 131, Asp 133, and His 187 are in direct interaction with the Fe(II). The model also shows Trp 178 located above His 187 and in the immediate vicinity. In fact, the distance between the Trp carbon at the fifth position, where hydroxylation is most likely, and the Fe(II) ion is only 4.7 Å in the predicted model after force-field based minimization. This compares favorably with the geometry in TauD where the distance between Fe(II) to Tyr 73, the tyrosine that becomes hydroxylated, is 6.5 Å [11].

3.4. Conclusions

When exposed to oxygen, α KG-Fe(II)AlkB forms a blue chromophore that closely resembles the spectrum of oxygen-exposed α KG-Fe(II)TfdA. On the basis of resonance Raman and mass spectrometric evidence, the TfdA chromophore previously was assigned to a LMCT band associated with OH-Trp coordination to Fe(III) [10]. LC/MS/MS evidence confirms that OH-Trp also is produced in AlkB and we propose that the spectrum

similarly derives from a OH-Trp/Fe(III) LMCT transition. Whereas the modified Trp in TfdA (Trp 113) immediately precedes a metal ligand (His 114), the AlkB modification (OH-Trp 178) is more distant from the closest ligand (His 187) in the sequence. Structure prediction efforts provide a robust three-dimensional model of AlkB that is consistent with Trp 178 being close to the metalcenter and capable of becoming hydroxylated.

Of interest, OH-Trp 178 also was identified in a control AlkB sample. We attribute this finding as indicating that self-hydroxylation can occur within the cell, where α KG, Fe(II), and oxygen are present, at least in the case of an overexpressing strain. Because oxygen exposure of Fe(II)AlkB does not yield a detectable blue chromophore, either the amount of OH-Trp is quite small in the sample or the chromophore only can be generated from unmodified AlkB, i.e. OH-Trp does not coordinate Fe(III) when previously modified protein is amended with Fe(II) and the metal is oxidized. These results suggest that anaerobic growth conditions could be used to help insure the production of fully active, unmodified protein.

The phenomenon of enzyme self-hydroxylation appears to be widespread in non-heme Fe(II) oxygenases. In addition to the hydroxylation of a Trp side chain noted above for AlkB and previously described for TfdA [10], a tyrosine residue is hydroxylated to form a catecholate derivative in TauD [11,12] and phenylalanine hydroxylation has been noted in both tyrosine hydroxylase [20,21] and the Y325F variant of phenylalanine hydroxylase [22]. Furthermore, both tyrosine and phenylalanine hydroxylation have been observed in various mutants of the R2 subunit of ribonucleotide reductase, a dinuclear iron protein [23–26]. The blue oxidized form of 4-hydroxyphenylpyruvate dioxygenase

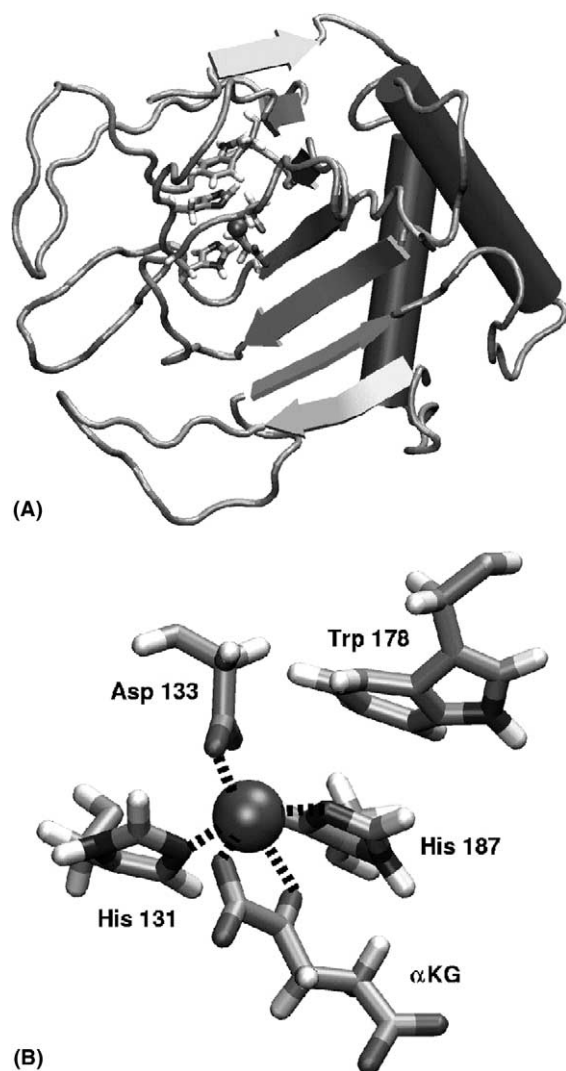


Fig. 4. Structure of AlkB determined by protein modeling. Panel A depicts the predicted fold of the monomer and reveals a β -jellyroll structure as found in other family members. Residues 1–15 are not included since their positions could not be reliably predicted. Panel B focuses on the region near the metalcenter and shows the three amino acid side chains that serve as ligands, the α KG, and the nearby Trp 178 that undergoes hydroxylation.

[27], assigned to a species possessing tyrosinate-Fe(III) LMCT transitions [28], might derive from analogous hydroxylation of an active site phenylalanine (as proposed in [29]) on the basis of the enzyme crystal structure which shows the absence of tyrosines, but presence of phenylalanines, in the vicinity of the metalcenter [30]. Biomimetic complexes designed to mimic the reactivity of α KG-dependent dioxygenases also undergo self-hydroxylation chemistry involving a ligand phenyl group [31,32]. In summary, the hydroxylation chemistry of several enzymes and model compounds is consistent with the generation of a highly reactive intermediate that oxidizes an aromatic substituent when the primary substrate is absent. It remains unclear whether the aberrant enzymatic reactions of AlkB and these other

systems may benefit the proteins by protecting them from more harmful oxidative reactions such as backbone cleavage reactions (as observed in aminocyclopropane carboxylate oxidase [33]).

4. Abbreviations

α KG	α -ketoglutarate or 2-oxoglutarate
EDTA	ethylenediaminetetraacetic acid
OH-Trp	hydroxytryptophan
LC/MS/MS	liquid chromatography coupled to tandem mass spectrometry/mass spectrometry
LMCT	ligand-to-metal charge-transfer
MLCT	metal-to-ligand charge-transfer
UV-Vis	ultraviolet-visible
2,4-D	2,4-dichlorophenoxyacetic acid

Acknowledgements

We thank Brett Phinney for assistance with the mass spectrometry and John McCracken for comments. This work was supported by National Institute of Health grants GM063584 (to R.P.H.) and GM54065 (to J.M.), and by the Michigan State University Agricultural Experiment Station.

References

- [1] H. Kataoka, Y. Yamamoto, M. Sekiguchi, *J. Bacteriol.* 153 (1983) 1301–1307.
- [2] S.C. Trewick, T.F. Henshaw, R.P. Hausinger, T. Lindahl, B. Sedgwick, *Nature* 419 (2002) 174–178.
- [3] P.O. Falnes, R.F. Johansen, E. Seeberg, *Nature* 419 (2002) 178–182.
- [4] P.A. Aas, M. Otterlei, P.O. Falnes, C.B. Vagbe, F. Skorpen, M. Akbari, O. Sundheim, M. Bjoras, G. Slupphaug, E. Seeberg, H.E. Krokan, *Nature* 421 (2003) 859–863.
- [5] T. Duncan, S.C. Trewick, P. Koivisto, P.A. Bates, P.A. Lindahl, B. Sedgwick, *Proc. Natl. Acad. Sci. USA* 99 (2002) 16660–16665.
- [6] A.G. Prescott, M.D. Lloyd, *Nat. Prod. Rep.* 17 (2000) 367–383.
- [7] J.C. Price, E.W. Barr, B. Tirupati, J.M. Bollinger Jr., C. Krebs, *Biochemistry* 42 (2003) 7497–7508.
- [8] J.-U. Rohde, J.-H. In, M.H. Lim, W.W. Brennessel, M.R. Bukowski, A. Stubna, E. Münck, L. Que Jr., *Science* 299 (2003) 1037–1039.
- [9] M.H. Lim, J.-U. Rohde, A. Stubna, M.R. Bukowski, M. Costas, R.Y.N. Ho, E. Münck, W. Nam, L. Que Jr., *Proc. Natl. Acad. Sci. USA* 100 (2003) 3665–3670.
- [10] A. Liu, R.Y.N. Ho, L. Que Jr., M.J. Ryle, B.S. Phinney, R.P. Hausinger, *J. Am. Chem. Soc.* 123 (2001) 5126–5127.
- [11] M.J. Ryle, A. Liu, R.B. Muthukumar, R.Y.N. Ho, K.D. Koehntop, J. McCracken, L. Que Jr., R.P. Hausinger, *Biochemistry* 42 (2003) 1854–1862.
- [12] M.J. Ryle, K.D. Koehntop, A. Liu, L. Que Jr., R.P. Hausinger, *Proc. Natl. Acad. Sci. USA* 100 (2003) 3790–3795.

- [13] S. Dinglay, S.C. Trewick, T. Lindahl, B. Sedgwick, *Genes Develop.* 14 (2000) 2097–2105.
- [14] K. Ginalski, A. Elofsson, D. Fisher, L. Rychlewski, *Bioinformatics* 19 (2003) 1015–1018.
- [15] K. Ginalski, J. Pas, L.S. Wyrwicz, M. von Grotthuss, J.M. Bujnicki, L. Rychlewski, *Nucl. Acids Res.* 31 (2003) 3804–3807.
- [16] M. Feig, J. Karanicolas, C.L. Brooks III, *J. Molec. Graphics Modeling* (2004) (in press).
- [17] J. Skolnick, A. Kolinski, A.R. Ortiz, *J. Mol. Biol.* 265 (1997) 217–241.
- [18] M. Feig, C.L. Brooks III, *Proteins* 49 (2002) 232–245.
- [19] B.R. Brooks, R.E. Bruccoleri, B.D. Olafson, D.J. States, S. Swaminathan, M. Karplus, *J. Comp. Chem.* 4 (1983) 187–217.
- [20] K.E. Goodwill, C. Sabatier, R.C. Stevens, *Biochemistry* 37 (1998) 13437–13445.
- [21] H.R. Ellis, S.C. Daubner, R.I. McCulloch, P.F. Fitzpatrick, *Biochemistry* 38 (1999) 10909–10914.
- [22] S.D. Kinzie, M. Thevis, K. Ngo, J. Whitelegge, J.A. Loo, M.M. Abu-Omar, *J. Am. Chem. Soc.* 125 (2003) 4710–4711.
- [23] M. Ormö, F. deMaré, K. Regnström, A. Aberg, M. Sahlin, J. Ling, T.M. Loehr, J. Sanders-Loehr, B.-M. Sjöberg, *J. Biol. Chem.* 267 (1992) 8711–8714.
- [24] M. Ormö, K. Regnström, Z. Wang, L. Que Jr., M. Sahlin, B.-M. Sjöberg, *J. Biol. Chem.* 270 (1995) 6570–6576.
- [25] D.T. Logan, F. deMaré, B.O. Persson, A. Slaby, B.-M. Sjöberg, P. Nordlund, *Biochemistry* 37 (1998) 10798–10807.
- [26] J. Baldwin, W.C. Voegtli, N. Khidekel, P. Moënne-Loccoz, C. Krebs, A.S. Pereira, B.A. Ley, B.H. Huynh, T.M. Loehr, P.J. Riggs-Gelasco, A.C. Rosenzweig, J.M. Bollinger Jr., *J. Am. Chem. Soc.* 123 (2001) 7017–7030.
- [27] S. Lindstedt, M. Rundgren, *J. Biol. Chem.* 257 (1982) 11922–11931.
- [28] F.C. Bradley, S. Lindstedt, J.D. Lipscomb, L. Que Jr., A.L. Roe, M. Rundgren, *J. Biol. Chem.* 261 (1986) 11693–11696.
- [29] M.J. Ryle, R.P. Hausinger, *Curr. Opinion Chem. Biol.* 6 (2002) 193–201.
- [30] L. Serre, A. Sailland, D. Sy, P. Boudec, A. Rolland, E. Pebay-Peyroula, C. Cohen-Addad, *Structure* 7 (1999) 977–988.
- [31] E.R. Hegg, R.Y.N. Ho, L. Que Jr., *J. Am. Chem. Soc.* 121 (1999) 1972–1973.
- [32] M.P. Mehn, K. Fujisawa, E.L. Hegg, L. Que Jr., *J. Am. Chem. Soc.* 124 (2003) 7828–7842.
- [33] Z. Zhang, J.N. Barlow, J.E. Baldwin, C.J. Schofield, *Biochemistry* 36 (1997) 15999–16007.